Available online at www.sciencedirect.com
ScienceDirect
International Journal of Heat and Mass Transfer 50 (2007) 1049–1060
International Journal of HEAT and MASS TRANSFER
www.elsevier.com/locate/ijhmt

# Flow pattern transition instability during flow boiling in a single microchannel

Cheol Huh [a], Jeongbae Kim [b], Moo Hwan Kim [a,*]

[a] Department of Mechanical Engineering, Pohang University of Science and Technology, San 31, Hyoja-dong, Namgu, Pohang, Kyoungbuk 790-784, Republic of Korea
[b] New and Renewable Energy Research Department, KIER (Korea Institute of Energy Research), 71-2, Jang-dong, Yuseong-gu, Daejeon 305-343, Republic of Korea

Received 26 September 2005; received in revised form 8 June 2006
Available online 13 October 2006

**Abstract**

We studied the unique characteristics of flow boiling in a single microchannel, including the periodic pressure drop, mass flow rate, and temperature fluctuations, in terms of a long time period. Experiments were conducted using a single horizontal microchannel and deionized water to study boiling instabilities at very small mass and heat flow rate conditions. A Polydimethylsiloxane (PDMS) rectangular single microchannel had a hydraulic diameter of 103.5 μm and a length of 40 mm. A series of piecewise serpentine platinum microheaters were fabricated on the inner bottom wall of the rectangular microchannel to supply thermal energy to the test fluid. Real-time flow visualizations of the flow pattern inside the microchannel were performed simultaneously with measurements of the experimental parameters. Tests were performed for mass fluxes of 170 and 360 kg/m$^2$ s and heat fluxes of 200–530 kW/m$^2$. The test results showed that the heated wall temperature, pressure drop, and mass flux all fluctuated with a long period and large amplitude. These periodic fluctuations exactly matched the transition of two alternating flow patterns inside the microchannel: a bubbly/slug flow and an elongated slug/semi-annular flow. Therefore, the flow pattern transition instability in the single microchannel caused a cyclic behavior of the wall temperature, pressure drop, and mass flux, and this behavior had a very long period (100–200 s) and large amplitude.


*Keywords:* Two-phase instability; Microchannel; Two-phase flow; Flow pattern transition; Flow boiling

## 1. Introduction

Flow instabilities are undesirable in boiling two-phase microchannel systems. Flow oscillations may affect the heat transfer and fluid flow characteristics, possibly resulting in wall temperature and heat flux oscillations, or they may induce dryout. Heat transfer and fluid flow in microscale channels are used in many applications, including microchannel heat sinks and microfluidic devices. In addition, two-phase microchannel heat sinks are one of the strongest candidates for heat removal devices in high heat flux environments by virtue of their large surface area to volume ratio, compact dimensions, and low flow rate requirements. However, two-phase flow instabilities often appear in boiling process systems in which two-phase flow is involved. Yadigaroglu [1] noted that two-phase flow instabilities generated by unstable flow patterns, particularly slug flow, could amplify flow disturbances and lead to dryout. Therefore, pressure and flow rate oscillations in microchannels should be identified and prevented to ensure safe operations. Bergles [2] and Boure et al. [3] noted that sustained flow oscillations may induce forced mechanical vibrations of components or system control problems. Flow oscillations can affect the local heat transfer

* Corresponding author. Tel.: +82 54 279 2165; fax: +82 54 279 3199.
*E-mail addresses:* dratom@postech.ac.kr (C. Huh), mhkim@postech.ac.kr (M.H. Kim).

0017-9310/$ - see front matter © 2006 Elsevier Ltd. All rights reserved.
doi:10.1016/j.ijheatmasstransfer.2006.07.027

**Nomenclature**

| | | | |
|---|---|---|---|
| $Co$ | confinement number, $\frac{\left(\frac{\sigma}{g\Delta\rho}\right)^{1/2}}{D_h}$ (–) | $q$ | heat flow rate (W) |
| $D_h$ | hydraulic diameter (m) | $q''$ | heat flux (kW/m$^2$) |
| $G$ | mass flux (kg/m$^2$ s) | $T$ | temperature (°C) |
| $H$ | thickness (m) | $t$ | time (s) |
| $I$ | electric current (A) | $u$ | experimental uncertainty (–) |
| $i$ | enthalpy (kJ/kg) | $V$ | electric voltage (V) |
| $\Delta i_{in}$ | enthalpy difference due to inlet subcooling (kJ/kg) | $W$ | width (m) |
| | | *Subscripts* | |
| $i_{fg}$ | heat of vaporization (kJ/kg) | bw | bottom wall of heater |
| $k$ | thermal conductivity (W/mK) | ch | channel |
| $L$ | length (m) | h | heater |
| $\dot{m}$ | mass flow rate (kg/s) | loss | heat losses |
| $P$ | pressure (kPa) | $n$ | section element (see Fig. 3) |
| $\Delta P$ | pressure drop (kPa) | w | heated wall |
| $Q$ | volume flow rate (ml/min) | | |
| $Re$ | Reynolds number, $\frac{GD_h}{\mu}$ (–) | | |

performance, possibly resulting in oscillatory wall temperatures or inducing a critical-heat flux. Kandlikar [4] also remarked that flow instabilities in mini/microchannel systems are a concern in the design of microchannel evaporators.

Recently, a few published studies have reported pressure-drop oscillations and hydrodynamic instabilities of flow boiling in microchannels. Zhang et al. [5] performed boiling experiments using deionized water in 113 μm silicon microchannels. They observed bubble inceptions and measured the temperature variations of the channel wall using the resistance change of seven boron doped silicon thermometers. They found that the 4–5 Hz resistance fluctuation frequencies measured by the thermometers agreed well with the bubble formation frequencies.

Kandlikar et al. [6] observed the flow patterns of boiling in six 60-mm-long parallel channels with 1-mm hydraulic diameter and reported pressure fluctuations with 1 Hz frequencies that were attributed to the boiling phenomena, specifically the evolution of the vapor. Flow reversals were observed due to growth of slug bubbles in the microchannels. The vapor interface moved in a direction counter to the bulk fluid flow, and a pressure-drop fluctuations with periods of a few seconds were also observed. Recently, Kandlikar [7] noted a similarity between flow boiling in microchannels and nucleate boiling. Thus, flow boiling in microchannels can be treated as a similar process to the bubble ebullition cycle in pool boiling.

Qu and Mudawar [8,9] conducted experiments on flow boiling of water in 21 parallel 231-μm-wide and 713-μm-high microchannels at mass fluxes ranging from 135 to 400 kg/m$^2$ s with heat fluxes up to 1300 kW/m$^2$. They encountered two types of two-phase hydrodynamic instabilities in parallel microchannels: pressure-drop oscillations and parallel channel instabilities. The pressure-drop oscillations, which had 20-s periods, were eliminated by throttling the upstream flow of the test section, or in other words, by adding system stiffness.

Hetsroni et al. [10] performed experiments on flow boiling of Vertrel XF in 21 parallel silicon triangular microchannels with a base of 250 μm. They observed 1-2-s oscillations of the pressure drop and outlet fluid temperature. Recently, Hetsroni et al. [11] reported an alternating occurrence of single-phase liquid flow and two-phase flow led to pressure-drop fluctuations with a short period. They explained the fluctuation phenomena based on bubble inception and growth behavior.

Wu and Cheng [12] performed experiments on flow boiling of water in 8–15 parallel silicon microchannels with trapezoidal cross-sections having hydraulic diameters of 82.8 and 158.8 μm. They showed that the wall temperature, fluid temperature, fluid pressure, and fluid mass flux varied with large amplitudes and long periods of 31 and 141 s in the small- and large-diameter systems, respectively. The temperatures and pressures fluctuations were in phase, but the pressure and mass flux fluctuations were out of phase. They reasoned that the out of phase fluctuations of pressure and mass flux triggered boiling onset oscillations [13] that sustained the fluctuations. Wu and Cheng [14] performed experiments on flow boiling of water in eight parallel silicon microchannels with trapezoidal cross-sections having a hydraulic diameter of 186 μm. They observed three types of unstable boiling modes. The pressure and mass flux were out of phase for single-phase/two-phase alternating flow and boiling onset oscillations sustained the fluctuations.

Brutin and Tadrist [15] carried out experiments in a single vertical channel with a hydraulic diameter of 889 μm using *n*-pentane as a working fluid. They derived a stability map drawn using the outlet vapor quality and inlet Reynolds number, and reported that a slight increase of the exit vapor quality at Reynolds numbers lower than 1000 could be used to identify the unstable regime. Recently, Tadrist

[16] noted that static two-phase flow instabilities may appear in narrow channels with high confinement numbers ($Co > 1$).

In this study, we developed novel techniques and a new experimental apparatus to investigate boiling instabilities and related heat transfer mechanisms in a single microchannel. The new apparatus made it possible to observe flow patterns while simultaneously measuring the momentum and thermal transport parameters. The objective of this study was to conduct thorough experimental investigations of flow boiling instabilities, study the fluctuation behavior of flow boiling parameters such as pressure drop and mass flux, and determine the reason for boiling instabilities in a single microchannel.

## 2. Experiments

### 2.1. Experimental apparatus

The experimental apparatus consisted of three major subsystems: a working fluid loop, a flow visualization system, and a data acquisition system. Fig. 1 shows a schematic diagram of the flow loop, which was configured to supply deionized water to the test section. The inlet reservoir served as a deaeration chamber due to the constant-temperature-controlled hot plate that removed any dissolved gas. Deionized water was delivered to the test section by dual operation syringe pumps: one syringe discharged water to the test section and the opposite syringe simultaneously provided suction from the inlet reservoir to fill the syringe barrel. This configuration of the pumps produced a continuous pulsation-free supply of working fluid. Before reaching the test section, discharged water passed through a line filter with 2-μm screen meshes to remove solid particles that could cause contamination and/or blockage of the flow passage. To adjust the stiffness of the upstream fluid handling system, the test microchannel was located ahead of a metering valve. Yadigaroglu [1] noted inlet single-phase throttling stabilizes the boiling channels. During normal tests in the present experimental study, the metering valve remained in its fully open state. After the test section, the water returned to the outlet reservoir installed on the electronic balance. The mass flow of water was measured by reading the mass gradient with time from the electronic balance.

Two absolute pressure transducers and four type-T thermocouples were located in the fluid connection port to measure the inlet and outlet pressures and temperatures. A differential pressure transducer was installed between the inlet and outlet of the test section to measure the pressure drop across the test section. The heat losses from the test section to the outside were estimated using six miniature type-K thermocouples located beneath the heater substrate, corresponding to each microheater.

Finally, a high-speed CCD camera (up to 100,000 fps) with a microscope was installed above the test section to provide real-time visualization of the microchannel flow boiling behavior, such as bubble inception and growth, bubble flow, and vapor and liquid interaction at the interface.

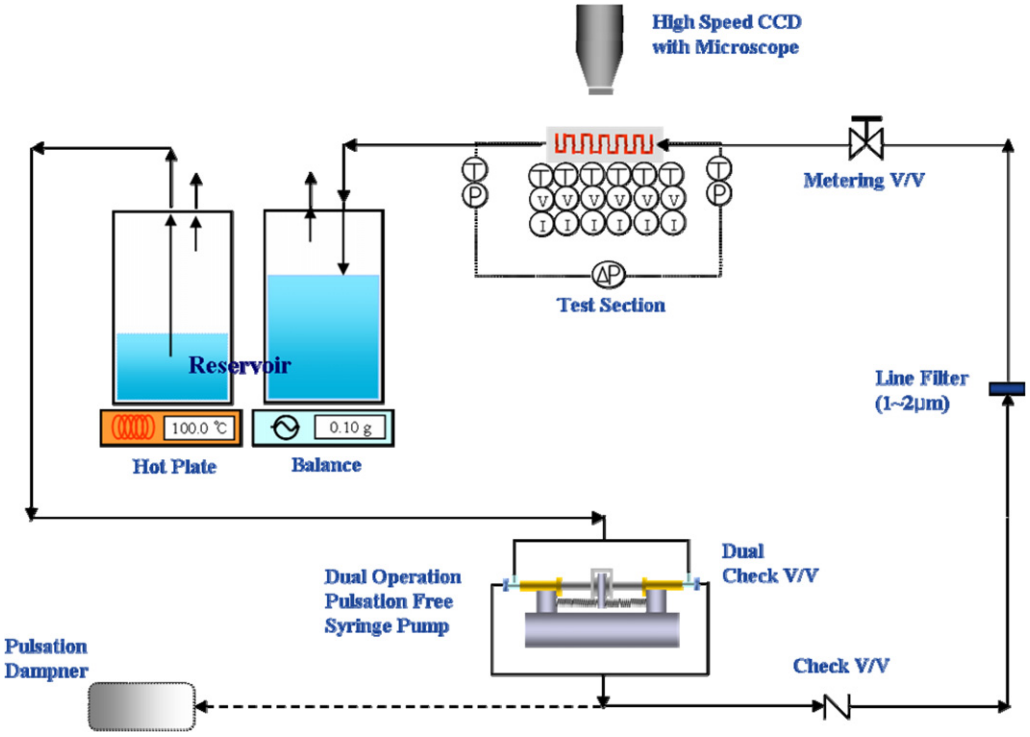


Fig. 1. Schematic diagram of the experimental apparatus.

### 2.2. Test section

The test section consisted of multiple microheaters and a single horizontal rectangular microchannel, as shown in Fig. 2. In total, six piecewise serpentine platinum microheaters, separated from each other were manufactured and spaced along the flow direction using a surface micromachining microelectro-mechanical systems (MEMS) technique. A 3000-Å-thick platinum layer was deposited on the bottom plate of the microchannel using an electron beam evaporator. The unwanted portions of the thin platinum layer were then removed using the lift-off method to leave only the microheaters. Yadigaroglu [1] and Yadigaroglu and Bergles [17] noted that both the heat capacity and transient heat conduction effects in the heater influence the flow stability by providing the necessary degree of freedom for variations of the heat flux to the coolant. However, the thin film platinum microheaters had low volumetric heat capacities and thermal masses due to their low heat capacities. The thin film microheaters also had low Biot numbers. Thus, it is reasonable to assume that the effects of conduction and thermal capacitance within the thin film microheaters were negligible compared to the convection effects across the fluid boundary layer.

Since platinum has a linear relationship between resistance and temperature, the platinum microheaters performed not only as heaters but also as temperature measurement sensors in the flow direction on the heated surface. The electrical voltage and current for each microheater were measured to obtain the heat input from the microheaters to the working fluid. Each microheater was calibrated in a constant temperature oil bath to quantify its temperature–resistance relationship.

A horizontal rectangular microchannel with a 103.5-μm hydraulic diameter and a 100-μm-wide and 107-μm-high channel cross-section was fabricated using the replica molding technique. The test microchannel had a length of 40 mm, which included an effective heating length of 30 mm. Polydimethylsiloxane (PDMS) was used as the structural material of the microchannel because of its good thermal and optical properties [18]. However, PDMS also has some unfavorable characteristics, such as high permeability to gas and porosity, which yield unexpected low temperature bubble formations [19,20]. Parylene film has a low permeability to moisture and gases such as nitrogen, oxygen, and carbon dioxide [21]. Therefore, to remove the undesirable effects of PDMS, both the inner and outer walls of the microchannel were coated with parylene C dimer (di-chloro-di-para-xylylene). Yadigaroglu and Bergles [17] noted that the heat storage in the channel wall could affect the enthalpy perturbation along the channel walls. They reported that the effect is probably important in the single-phase region because of the relative insensitivity of the boiling heat transfer coefficient to flow rate conditions. Even though the parylene-coated PDMS microchannel had a high heat capacity, it had a low volumetric heat capacity and thermal mass due to its low density compared to copper and stainless steel microchannels. Therefore, the transient heat storage and release in the microchannel wall could be neglected.

### 2.3. Test conditions and procedures

The experimental conditions are summarized in Table 1. Tests were performed for mass fluxes of 170 and 360 kg/m$^2$ s, and heat fluxes of 200–530 kW/m$^2$. Single-phase tests were performed before the two-phase experiments to check

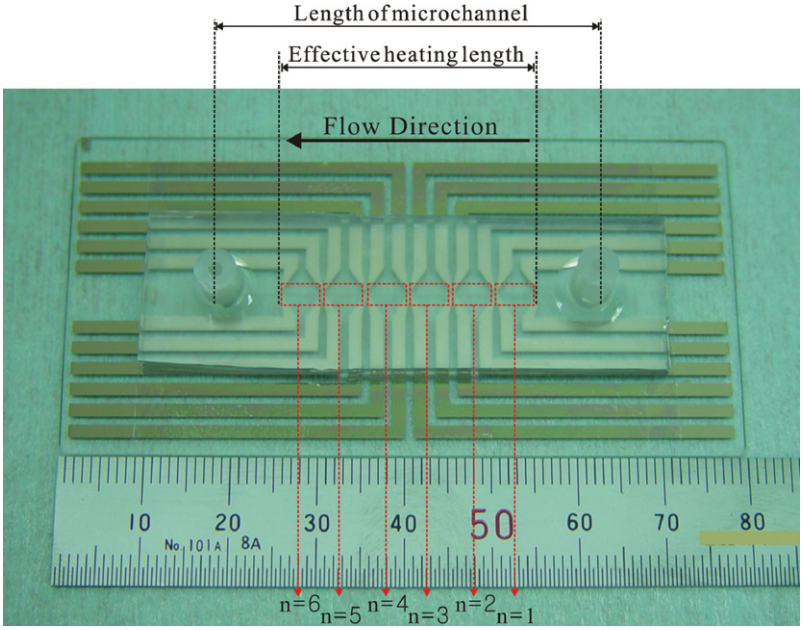


Fig. 2. Six serpentine microheaters with single microchannel.

Table 1
Experimental conditions

| | |
|---|---|
| Hydraulic diameter | 103.5 μm (width 100 μm, height 107.2 μm) |
| Test channel length | 40 mm |
| Effective heating length | 30 mm |
| Working fluid | Deionized water |
| Volume flow rate[a] | 0.01–0.02 ml/min |
| Mass flux | 170–360 kg/m$^2$ s |
| Reynolds number, $Re_{fo}$[b] | 19.2–38.3 |
| Heat flux | 200–530 kW/m$^2$ |

[a] Initial volume flow rate is determined at the single-phase inlet conditions.
[b] $Re_{fo}$ is the Reynolds number assuming that the total flow is liquid.

the reliability of the experimental systems. As a result, we determined the friction factor for single-phase liquid flow, which compared well to the value obtained using conventional theory.

Prior to conducting a test, the water in the inlet reservoir was deaerated by boiling to remove any dissolved gases. The components of the test flow loop were adjusted to provide the desired mass flux, inlet pressure, and differential pressure across the test section. After the flow rate and pressure became stable, the heater power was increased in small increments while the test loop components were adjusted to maintain the desired operating conditions.

### 2.4. Data reduction and experimental uncertainties

As shown in the schematic diagram of the test apparatus, six microheaters spaced along the flow direction were operated both as pre-heaters for the single-phase liquid and as main heaters for the two-phase mixture. Therefore, the microchannel could be divided into six sections along the flow direction, $n = 1$–6, from the entrance to the exit. Fig. 3 illustrates the six sections, each composed of a microheater and microchannel. The heat generated by Joule heating and the heat losses to the environment were taken into account to determine the heat flux from the microheater to the working fluid. The heat generation and heat loss from each microheater were calculated using

$$q_n = V_n I_n \tag{1}$$

$$q_{\mathrm{loss},n} = \frac{k_{\mathrm{bw},n}(T_{\mathrm{h},n} - T_{\mathrm{bw},n})}{H_{\mathrm{bw},n}} W_{\mathrm{ch},n} L_{\mathrm{ch},n} \tag{2}$$

Table 2
Experimental uncertainties

| | |
|---|---|
| Temperature | ±0.1 °C |
| Pressure | ±0.76 kPa |
| Differential pressure | ±0.34 kPa |
| Volume flow rate | ±0.1% |
| Heater voltage | ±0.3% |
| Heater current | ±0.5% |
| Heat flux | ±2.7–±3.1% |

The effective heat flux at the $n$th microheater/microchannel section was calculated from

$$q''_n = \frac{q_n - q_{\mathrm{loss},n}}{W_{\mathrm{ch},n} L_{\mathrm{ch},n}} \tag{3}$$

The experimental uncertainties of heat flux at each heater were determined using the Holman method [22] as follows:

$$\frac{u_{q''_n}}{q''_n} = \sqrt{\left(\frac{u_{q_n}}{q_n - q_{\mathrm{loss},n}}\right)^2 + \left(\frac{u_{q_{\mathrm{loss},n}}}{q_n - q_{\mathrm{loss},n}}\right)^2 + \left(\frac{u_{W_{\mathrm{ch},n}}}{W_{\mathrm{ch},n}}\right)^2 + \left(\frac{u_{L_{\mathrm{ch},n}}}{L_{\mathrm{ch},n}}\right)^2} \tag{4}$$

Accounting for all the instrumentation errors, the uncertainties for the heat fluxes were estimated at ±2.7 to ±3.1%. The estimated experimental uncertainties of the pressure, temperature, differential pressure, and flow rate are shown in Table 2.

## 3. Results and discussion

The tests were conducted for mass fluxes of 170 and 360 kg/m$^2$ s and heat fluxes of 200–530 kW/m$^2$, as summarized in Table 1. The inlet subcooled liquid was heated to saturation as it passed through the test section for low heat flux conditions. No oscillation or fluctuations were observed for single-phase flow. As the heat flux was further increased, inception and growth of bubbles occurred, and then temporal variation of the fluid pressure and wall temperatures was observed. We will focus on the results of two test cases in this paper: one with a mass flux of 179.8 kg/m$^2$ s and a heat flux 372.4 kW/m$^2$ for each heater, and another with a mass flux of 349.6 kg/m$^2$ s and a heat flux 487.5 kW/m$^2$.

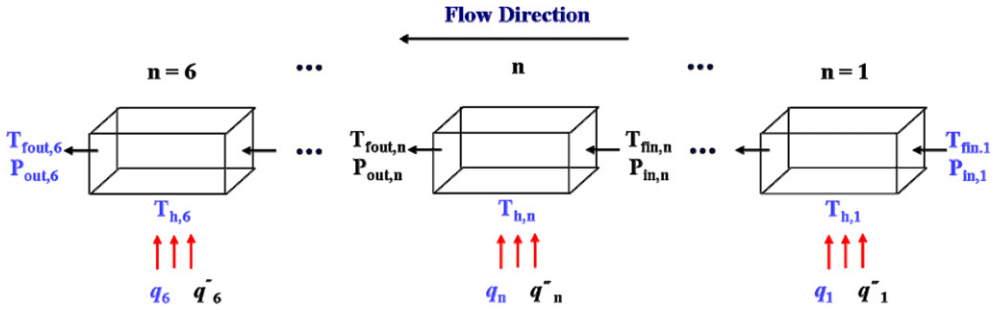


Fig. 3. Six sections of the microheater/microchannel.

### 3.1. Pressure drop and mass flux fluctuations

Fig. 4(a) and (b) show the pressure drop and mass flux fluctuations for a mass flux of 179.8 kg/m$^2$ s and a heat flux of 372.4 kW/m$^2$, which were the initial test conditions. The pressure drop fluctuated with a period of about 400 s and amplitude of 10 kPa. Since the outlet pressure of the test section remained constant at atmospheric pressure during the test, the pressure-drop behavior represented variations of the test section inlet pressure. These fluctuations had a very long period and large amplitude not observed in previous research. The mass flux fluctuated periodically with the same period as the pressure drop and an amplitude of 500 kg/m$^2$ s. In addition, the mass flux had a negative value at its lowest point, indicating flow reversal. A phase difference occurred between the pressure drop and mass flux fluctuations, and the mass flux increased suddenly at the highest inlet pressure. This phase difference may have been due to a pressure buildup at the inlet that increased until it reached a sufficient driving pressure to force the mass flow through the test section.

For the higher flow rate test case, with a mass flux of 349.6 kg/m$^2$ s and a heat flux of 487.5 kW/m$^2$, results similar to the low flow rate conditions were observed, as shown in Fig. 5(a) and (b). The fluctuation period of the pressure drop was about 210 s and the amplitude was 5.2 kPa. The amplitude of the mass flux fluctuation was 400 kg/m$^2$ s and the period of the mass flux fluctuation was the same as that of the pressure drop. Thus, the fluctuations had a shorter period and smaller amplitude than the lower flow rate cases, but a similar phase shift between the pressure drop and mass flux was observed. However, the relative amount of supplied heat for evaporation decreased with the increased mass flux, indicating that the fluctuations had a longer period and larger amplitude as the vapor quality increased. To verify the effect of vapor quality on the periodic fluctuations, tests were performed in which the heat flux was varied for a similar flow rate. As the supplied heat flux increased, the period of the fluctuations lengthened

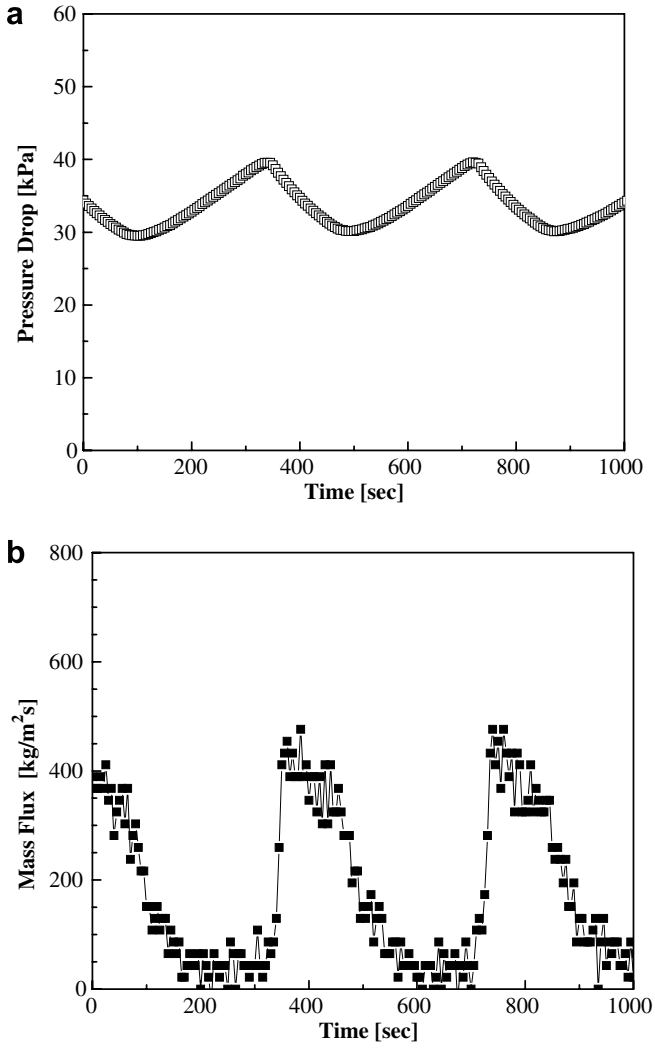


Fig. 4. Fluctuations of (a) pressure drop and (b) mass flux at $G =$ 179.8 kg/m$^2$ s, $q'' = 372.4$ kW/m$^2$.

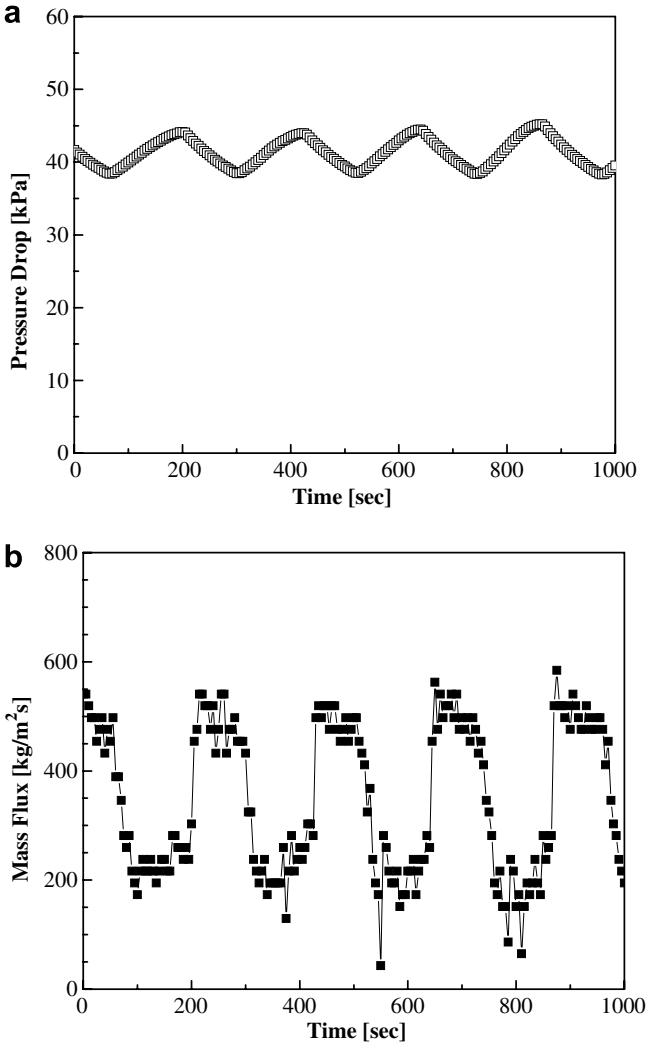


Fig. 5. Fluctuations of (a) pressure drop and (b) mass flux at $G =$ 349.6 kg/m$^2$ s, $q'' = 487.5$ kW/m$^2$.

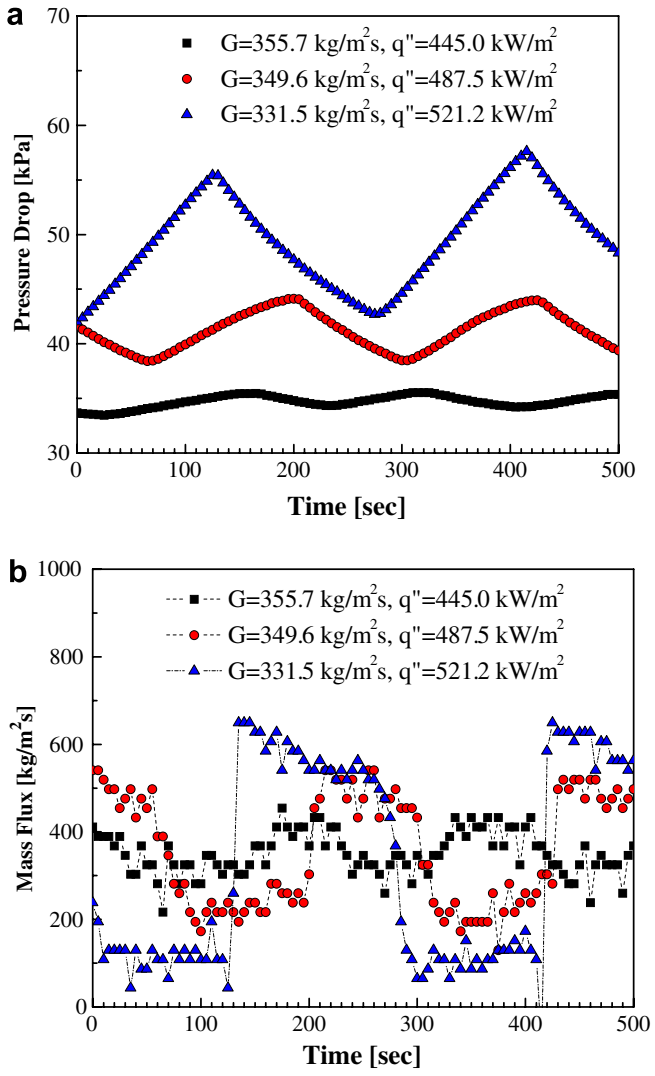


Fig. 6. Comparison of (a) pressure-drop fluctuations and (b) mass flux fluctuations.

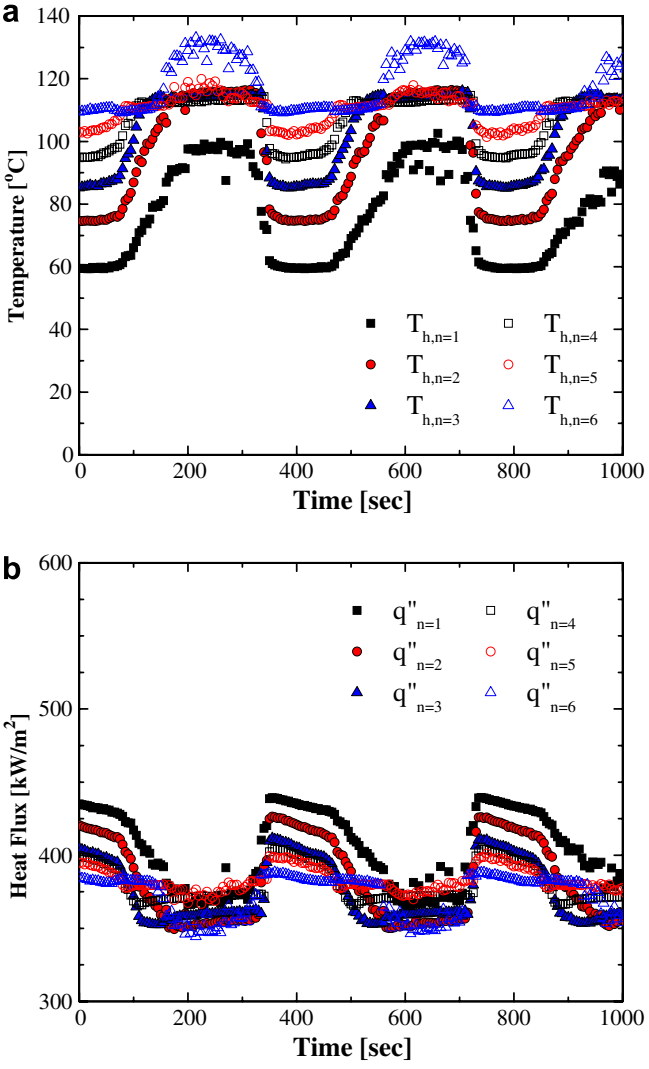


Fig. 7. Fluctuations of (a) wall temperature and (b) heat flux at $G = 179.8$ kg/m$^2$ s, $q'' = 372.4$ kW/m$^2$.

and the amplitude became larger, as shown in Fig. 6(a) and (b). Therefore, the extent of the unstable fluctuations increased as the boiling process proceeded, and the vapor quality consequently increased.

### 3.2. Temperature and heat flux fluctuations

Fig. 7(a) shows the variation in the heated wall temperature for a mass flux of 179.8 kg/m$^2$ s and a heat flux of 372.4 kW/m$^2$. In the single-phase region, $n = 1$–3, the wall temperature varied with an amplitude of 40 °C. This increased as the mass flux decreased and vice versa. At the highest differential pressure, the mass flow rate suddenly increased and the wall temperature decreased. Then the differential pressure gradually decreased and the wall temperature remained constant. At the lowest differential pressure, the mass flow rate continually decreased and the wall temperature increased. Then the differential pressure gradually increased due to the generation of more bubbles while the wall temperature remained constant. In the two-phase region, $n = 4$–6, the temperature fluctuations had an amplitude of 20 °C and showed the same variation trends as the single-phase region. The fluctuations in the wall temperature and mass flux were exactly out of phase whereas the heat flux fluctuated in phase with the mass flux, as shown in Fig. 7(b). The heat flux fluctuations had a large amplitude over $n = 1$–3 and a small amplitude over $n = 4$–6, similar to the wall temperature, while the period was the same as the mass flux. Once again, both wall temperature and heat flux exhibited similar fluctuations, as shown in Fig. 8(a) and (b), while the period and amplitude decreased with the vapor quality.

### 3.3. Visualization of periodic boiling

Visualizations of the flow patterns during the experiments were obtained simultaneously with the pressure, temperature, and heat input measurements. Figs. 9 and

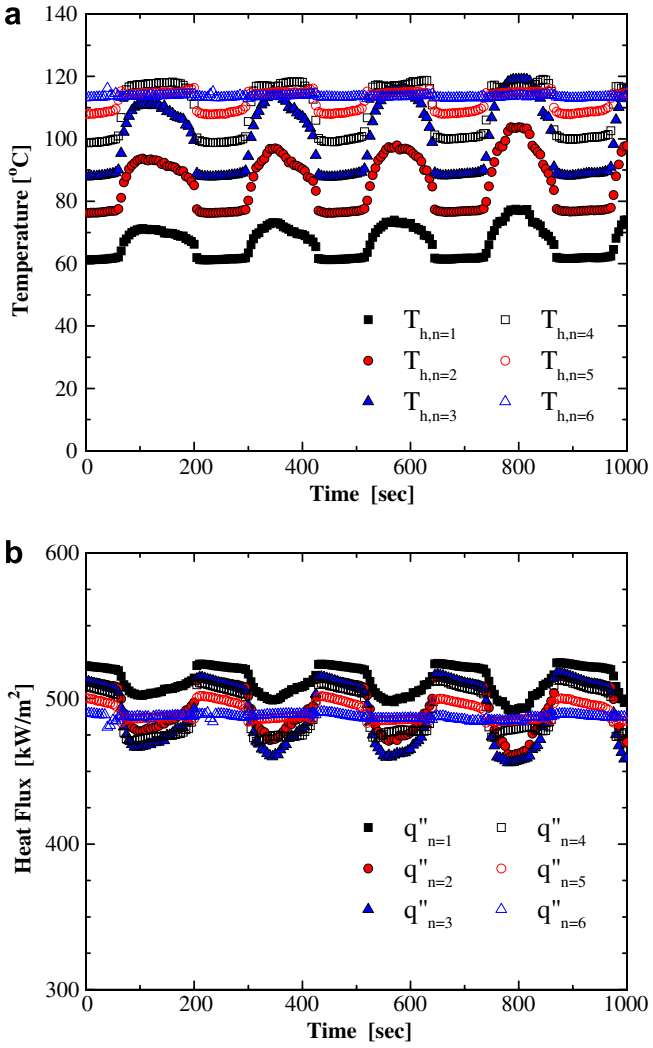


Fig. 8. Fluctuations of (a) wall temperature and (b) heat flux at $G = 349.6\ \mathrm{kg/m^2\,s}$, $q'' = 487.5\ \mathrm{kW/m^2}$.

10 show the flow patterns observed during the flow boiling experiments, which were taken with a high-speed CCD camera placed at the last microheater/microchannel section at $n = 6$ with a speed of 10,000 fps.

For the higher mass flux, with a lower wall temperature and higher heat flux states during the periodic variations, a bubbly/slug flow was observed, as shown in Fig. 9. Single bubbles began to be incepted in the middle of the test channel at $n = 4$–5, while more bubbles were incepted near the outlet region at $n = 6$. The bubbles grew to the channel width, moved downstream while growing in the flow direction, and finally formed slug and elongated bubbles within a few milliseconds. The elongated bubbles were a result of bubble growth due to the continual supply of heat, the confined flow passage, and the coalescence of single bubbles flowing along the channel. An animated movie of this behavior is shown in Movie 1 (see Electronic Annex 1 in Supplementary data). The bubbly/slug flow pattern was maintained when a lower wall temperature spanned the region $n = 5$–6. As the mass flux decreased, the wall temperatures increased, and more bubbles formed and grew to elongated slug bubbles. The elongated slug bubbles grew not only in the flow direction but also counter to the bulk fluid flow. Flow reversal or restriction occurred, causing the inlet pressure to increase as shown by the differential pressure variations in Figs. 4 and 5. Finally, the two-phase regions were filled with very long and fast elongated slugs that behaved like a semi-annular flow, as shown in Fig. 10. This elongated slug/semi-annular flow pattern was maintained when a higher wall temperature spanned the region $n = 4$–6. An animated movie of this flow pattern is shown in Movie 2 (see Electronic Annex 2 in Supplementary data). A short liquid zone between the long and fast elongated slugs that had a vapor core and liquid film was also observed. Fig. 11 shows the flow reversal and growth of the elongated bubbles/slugs in the opposite direction to the bulk fluid flow. An animated movie is shown in Movie 3 (see Electronic Annex 3 in Supplementary data).

Periodic flow pattern transitions, which consisted of alternating occurrences of the bubbly/slug flow shown in

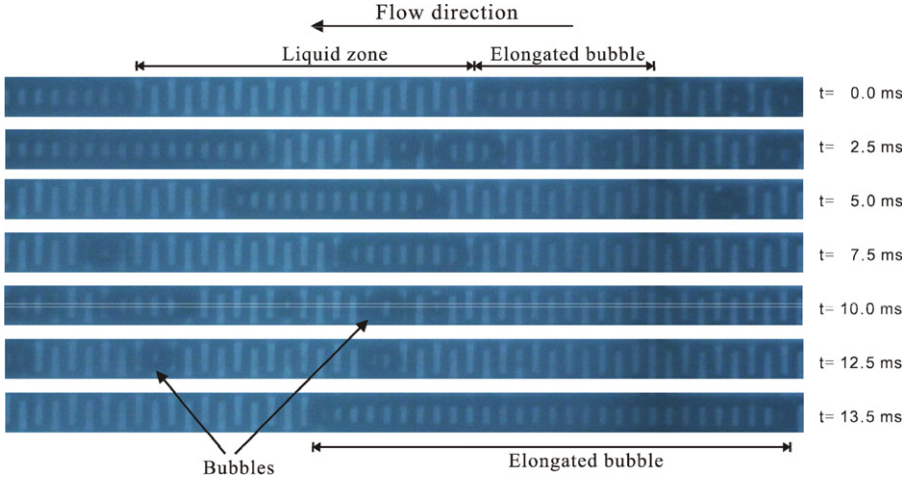


Fig. 9. Bubbly/slug flow at high mass flux, low wall temperature, and high heat flux conditions. (A related movie is shown in Movie 1.)

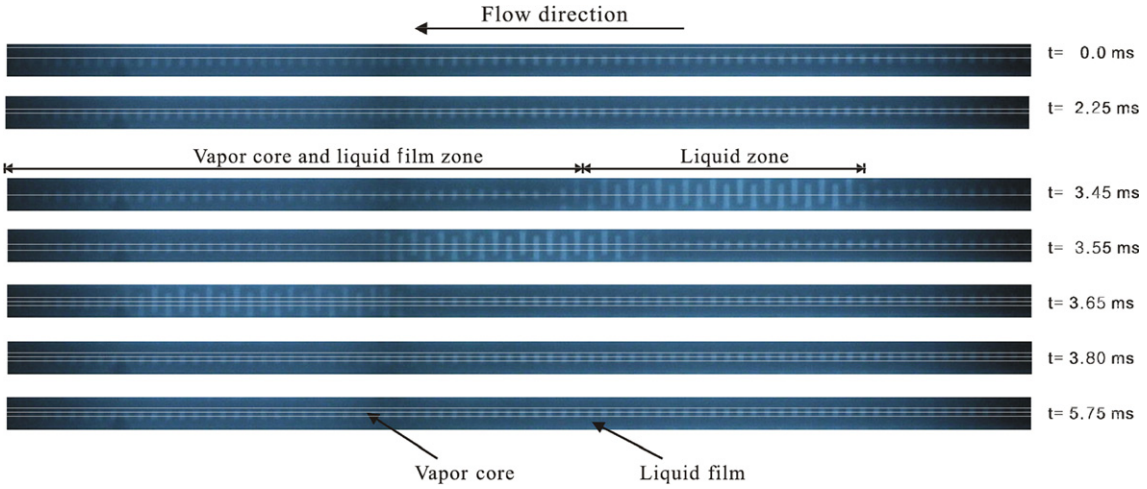


Fig. 10. Elongated slug/semi-annular flow at low mass flux, high wall temperature, and low heat flux conditions. (A related movie is shown in Movie 2.)

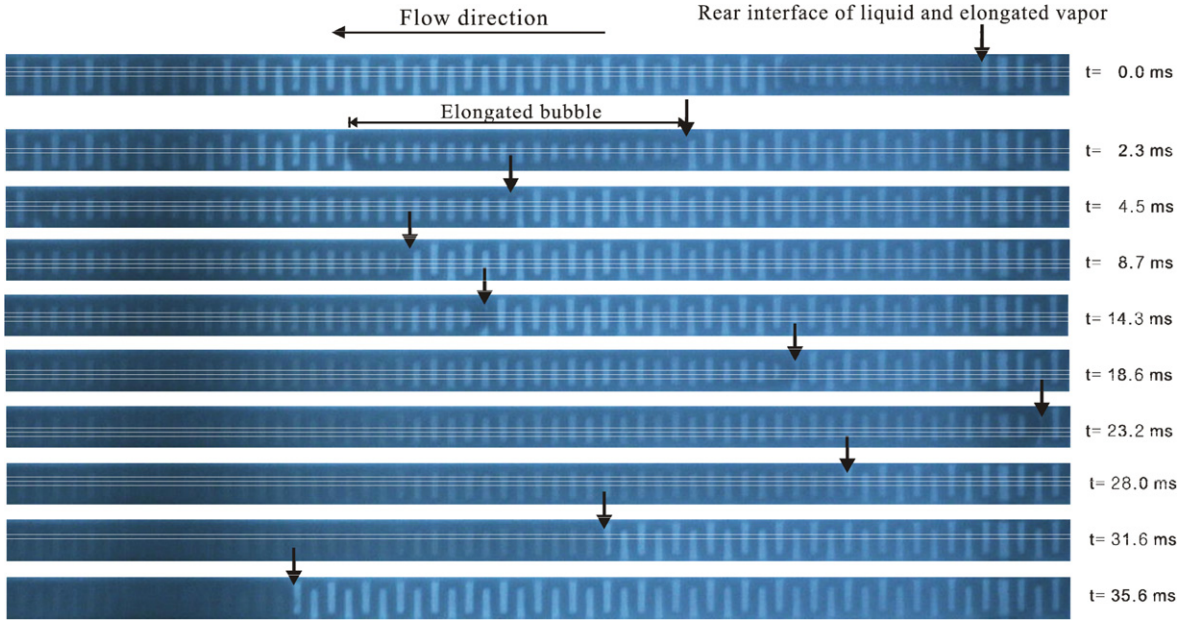


Fig. 11. Flow reversal due to the growth of the elongated bubble. (A related movie is shown in Movie 3.)

Fig. 9 and the elongated slug/semi-annular flow shown in Fig. 10, were observed during the pressure, temperature, and mass flux fluctuations. Movie 4 shows the flow pattern transitions from bubbly/slug flow to elongated slug/semi-annular flow captured at 30 fps at the last microheater/microchannel section (see Electronic Annex 4 in Supplementary data). These flow pattern transitions occurred for the lowest inlet pressure, decrease of the mass flux, increase of the wall temperature, and decrease of the heat flux. Movie 5 shows the flow pattern transitions from elongated slug/semi-annular flow to bubbly/slug flow (see Electronic Annex 5 in Supplementary data). These flow pattern transitions occurred for the highest inlet pressure, increase of the mass flux, decrease of the wall temperature, and increase of the heat flux.

## 4. Two-phase instabilities in a single microchannel

Many experimental and theoretical investigations of fluctuation or oscillation instabilities in conventional macro two-phase systems have been carried out. Flow instabilities can be classified as static instabilities, such as flow excursion, flow pattern transition instability, and bumping, or as dynamic instabilities, such as acoustic oscillations, density-wave oscillations, thermal oscillations, parallel channel instability, and pressure-drop oscillations [1–3].

Kandlikar et al. [6], Qu and Mudawar [8], Hetsroni et al. [10,11], and Wu and Cheng [12,14] reported flow boiling instabilities in parallel microchannel two-phase systems. However, the unusually long fluctuation periods of the

present study were not observed in previous work. In addition, when parallel channels are fed through a common inlet plenum, the channels oscillate while the flow in the remaining system remains constant. This is possible because the phases of the oscillations in the different channels adjust to stabilize the system [1]. Thus, the flow pattern transition instability of the present study is unique to flow boiling in a single microchannel. In addition, most of the previous studies [6,8,10,11] dealt with instabilities related to bubble inception and departure which have high frequencies.

Acoustic oscillations are characterized by high frequencies, with periods the same order of magnitude as the time required for a pressure wave to travel through the system [2]. Yadigaroglu [1] and Boure [3] noted that the commonly observed frequencies of acoustic oscillations were in the range of 10–100 Hz, which are higher than the frequencies observed in Section 3. Therefore, acoustic oscillations did not cause the unstable fluctuations in the present study.

Density-wave oscillations are caused by feedback between the flow rate, vapor generation rate, and pressure drop. Yadigaroglu and Bergles [17] noted that inlet flow fluctuations create enthalpy perturbations in the single-phase region, which reach the boiling region, where they are transformed into void fraction perturbations that finally create dynamic pressure-drop oscillations in the two-phase region. They proposed a map of density-wave oscillations with dimensionless enthalpy representing void and subcooling effects. In the present study, the dimensionless subcooling $\Delta i_{in}/i_{fg}$ was very small due to the small subcooling enthalpy difference and large heat vaporization. The dimensionless enthalpy $q/\dot{m}i_{fg}$ was also very small, as shown in Fig. 12. Therefore, density-wave oscillations did not cause the observed unstable fluctuations in the present study.

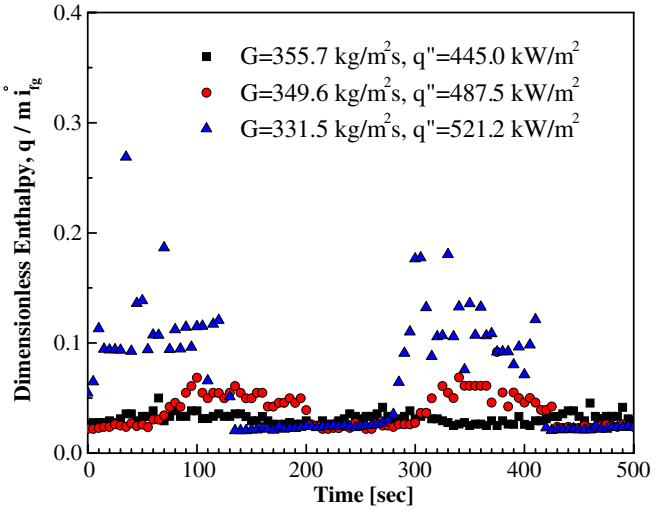


Fig. 12. Variations of the dimensionless enthalpy, $\frac{q}{\dot{m}i_{fg}}$.

Pressure-drop oscillations have a low frequency as low as 0.1 Hz. They occur in boiling two-phase systems with a compressible volume upstream of or within the heated section. They can be virtually eliminated by throttling the flow immediately upstream of the test channel [8]. To evaluate the effect of the upstream fluid handling system, we performed experiments in which the length of tubing between the syringe pump and the test section was varied from a half to two times of the normal length. No outstanding differences were observed, but the pressure drop, wall temperature, and mass flux fluctuations still appeared. The pressure-drop fluctuations were also not eliminated by throttling the working fluid flow.

Ding et al. [23] reported experimental dynamic instabilities of boiling two-phase R-11 flow in a single horizontal channel. They classified their results according to pressure drop, density-wave, and thermal oscillations. But the flow behavior was different to that of the present instabilities. Nakajima et al. [24] observed long period (30–60 s) and large amplitude (0–300 kg/m$^2$ s) mass flux fluctuations in a two-phase loop with a periodic discharge in which steam bubbles coalesced in a segment of horizontal piping. Although the coalescence of bubbles in the outlet was observed in the present study, the discharge frequency was totally different from the frequency of the pressure, temperature, and mass flux fluctuations.

In the present study, fluctuations with a very long period (100–200 s) and large amplitude were observed in single microchannel flow boiling. Since the parallel channel instabilities, such as uneven flow distribution, header-channel interactions, and channel-to-channel interactions between neighboring channels, were fundamentally removed, fluctuations in a two-phase system solely due to boiling phenomena were measured and visualized.

Flow pattern transition instabilities have been postulated to occur when flow conditions are close to the transition point between bubbly and annular flow [3]. It is evident that a phase shift occurred between the pressure drop and mass flux while the wall temperature and heat flux were exactly in phase, as shown in Figs. 4–8. As the mass flux increased, the wall temperature decreased and elongated slug/semi-annular flow changed to bubbly/slug flow due to insufficient bubble generation and growth. The pressure drop, which represented the inlet pressure, decreased due to the release of the built-up pressure at the inlet. As more bubbles incepted and departed, the departing bubbles grew into elongated bubbles that clogged the channel, causing the differential pressure to increase and the mass flow rate to decrease. As the mass flux decreased, the wall temperatures increased and elongated slugs grew more violently both in and opposite to the flow direction. An increase in the bubble population in bubbly/slug flow may change the flow pattern to elongated slug/semi-annular flow. The differential pressure increased until sufficient pressure had built-up at the inlet and the cyclic flow pattern transitions were repeated. Thus, variations of temperature, pressure, and mass flux exactly

matched the flow pattern transitions between bubbly/slug and elongated slug/semi-annular flow, as shown in Figs. 4–10. Therefore, the flow pattern transition instability in a single microchannel caused a cyclic behavior of the wall temperature, pressure drop, and mass flux, and this behavior had a very long period and large amplitude.

At present, no definite analytical method exists to predict the stability of flow patterns, and it is unclear whether the flow pattern transition is the cause or the consequence of a density-wave or pressure drop oscillation [1,2]. Bergles et al. [25], however, noted that it was possible the pressure-drop oscillation to occur due to the internal compressible volume of very long channel ($L/D_h > 150$). Microchannels, such as the one examined in the present study, may well exceed this length so that the internal volume filled with vapor can affect the flow stability of two-phase flow. In addition, Bergles et al. [26] reported that the flow pattern instability, which is internal to the heated section, is particularly important to the low pressure, unstable slug flow pattern.

## 5. Conclusions

In this study, experiments were performed to simultaneously measure and visualize flow boiling of water in a single microchannel with a hydraulic diameter of 103.5 μm. Tests were performed at mass fluxes of 170 and 360 kg/m$^2$ s and heat fluxes of 200–530 kW/m$^2$. The key findings of this study are as follows.

(1) Flow boiling fluctuations with a very long period and large amplitude were observed. Both the pressure drop and mass flux had these fluctuations, but a phase shift occurred between them that controlled the flow patterns.
(2) The fluctuation of wall temperature and heat flux had the same period as that of the mass flux. The wall temperature and mass flux fluctuations were exactly out of phase while the heat and mass flux fluctuations were exactly in phase. Variations in the wall temperature controlled the flow patterns.
(3) The variation in temperatures, pressure, and mass flux exactly matched the flow pattern transitions between bubbly/slug flow and elongated slug/semi-annular flow. The flow pattern transition instabilities in the single microchannel caused the cyclic behavior of the wall temperature, pressure drop, and mass flux.
(4) As the supplied heat flux and vapor quality increased, the period of the unstable fluctuations lengthened and the amplitude also increased.

## Acknowledgments

This research was supported by the Program for the Training of Graduate Students in Regional Innovation, which was conducted by the Ministry of Commerce, Industry, and Energy of the Korean government.

## Appendix A. Supplementary data

Supplementary data associated with this article can be found, in the online version, at doi:10.1016/j.ijheatmasstransfer.2006.07.027.

## References

[1] G. Yadigaroglu, Two-phase flow instabilities and propagation phenomena, in: J.M. Delhaye, M. Giot, M.L. Riethmuller (Eds.), Thermohydraulics of Two-Phase systems for Industrial Design and Nuclear Engineering, Hemisphere, Washington DC, 1981, pp. 353–403.
[2] A.E. Bergles, Review of instability in two-phase systems, in: S. Kakac, F. Mayinger (Eds.), Two-Phase Flows and Heat Transfer, vol. 1, Hemisphere, Washington DC, 1977, pp. 383–422.
[3] J.A. Boure, A.E. Bergles, L.S. Tong, Review of two-phase flow instability, Nucl. Eng. Des. 25 (1973) 165–192.
[4] S.G. Kandlikar, Fundamental issues related to flow boiling in minichannels and microchannels, Exp. Thermal Fluid Sci. 26 (2002) 389–407.
[5] L. Zhang, J. Koo, L. Jiang, K.E. Goodson, J.G. Santiago, T.W. Kenny, Study of boiling regimes and transient signal measurements in microchannels, in: Proc. Transducers'01, Munich, Germany, 2001, pp. 1514–1517.
[6] S.G. Kandlikar, M.E. Steinke, S. Tian, L.A. Campbell, High-speed photographic observation of flow boiling of water in parallel minichannels, in: Proc. National Heat Transfer Conference, ASME, Anaheim, CA, 2001, pp. 675–684.
[7] S.G. Kandlikar, Heat transfer mechanisms during flow boiling in microchannels, J. Heat Transfer 126 (2004) 8–16.
[8] W. Qu, I. Mudawar, Measurement and prediction of pressure drop in two-phase microchannel heat sinks, Int. J. Heat Mass Transfer 46 (2003) 2737–2753.
[9] W. Qu, I. Mudawar, Flow boiling heat transfer in two-phase microchannel heat sinks—I. Experimental investigation and assessment of correlation methods, Int. J. Heat Mass Transfer 46 (2003) 2755–2771.
[10] G. Hetsroni, A. Mosyak, Z. Segal, G. Ziskin, A uniform temperature heat sink for cooling of electronic devices, Int. J. Heat Mass Transfer 45 (2002) 3275–3286.
[11] G. Hetsroni, A. Mosyak, E. Pogrebnyak, Z. Segal, Explosive boiling of water in parallel microchannels, Int. J. Heat Mass Transfer 31 (2005) 371–392.
[12] H.Y. Wu, P. Cheng, Visualization and measurements of periodic boiling in silicon microchannels, Int. J. Heat Mass Transfer 46 (2003) 2603–2614.
[13] Q. Wang, X.J. Cheng, S. Kakac, Y. Ding, Boiling onset oscillation: a new type of dynamic instability in a forced-convection upflow boiling system, Int. J. Heat Fluid Flow 17 (1996) 418–423.
[14] H.Y. Wu, P. Cheng, Boiling instability in parallel silicon microchannels at different heat flux, Int. J. Heat Mass Transfer 47 (2004) 3631–3641.
[15] D. Brutin, L. Tadrist, Pressure drop and heat transfer analysis of flow boiling in a minichannels: influence of the inlet condition on two-phase flow instability, Int. J. Heat Mass Transfer 47 (2004) 2365–2377.
[16] L. Tadrist, Review on two-phase flow instabilities in narrow spaces, in: Proc. ECI International Conference on Heat Transfer and Fluid Flow in Microscale, ECI, Castelvecchio Pascoli, Italy, 2005, CD-ROM, # paper KL4.
[17] G. Yadigaroglu, A.E. Bergles, Fundamental and higher-mode density-wave oscillations in two-phase flow, J. Heat Transfer 94 (1972) 189–195.
[18] S.K. Sia, G.M. Whitesides, Microfluidic devices fabricated in poly(dimethylsiloxane) for biological studies, Electrophoresis 24 (2003) 3563–3576.

[19] J.N. Lee, C.M. Park, G.M. Whitesides, Solvent compatibility of poly(dimethylsiloxane)-based microfluidic devices, Anal. Chem. 75 (2003) 6544–6554.
[20] T.C. Merkel, V.I. Bondar, K. Nagai, B.D. Freeman, I. Pinnau, Gas sorption, diffusion, and permeation in poly(dimethylsiloxane), J. Polym. Sci. 38 (2000) 415–434.
[21] Y.S. Shin, K. Cho, S.H. Lim, S. Chung, S. Park, C. Chung, D. Han, J.K. Chang, PDMS-based miro PCR chip with Parylene coating, J. Micromech. Microeng. 13 (2003) 768–774.
[22] J.P. Holman, Experimental Methods for Engineers, seventh ed., McGraw-Hill, 2001.
[23] Y. Ding, S. Kakac, X.J. Chen, Dynamic instabilities of boiling two-phase flow in a single horizontal channel, Exp. Thermal Fluid Sci. 11 (1995) 327–342.
[24] I. Nakajima, A. Kawada, K. Fukuda, T. Kobori, An experimental study on the instability induced by voiding from a horizontal pipe line, ASME paper 75-WA/HT-20, 1975.
[25] A.E. Bergles, J.H. Lienhard, G.E. Kendall, P. Griffith, Boiling and evaporation in small diameter channels, Heat Transfer Eng. 24 (2003) 18–40.
[26] A.E. Bergles, R.F. Lopina, M.P. Fiori, Critical-heat-flux and flow pattern observations for low-pressure water flowing in tubes, J. Heat Transfer 89 (1967) 69–74.